RSC Advances

PAPER

View Article Online
View Journal | View Issue

Cite this: *RSC Adv.*, 2020, **10**, 29659

Heteroleptic manganese compounds as potential precursors for manganese based thin films and nanomaterials†

Sunju Lee,[a] Ga Yeon Lee,[a] Chang Gyoun Kim,[ab] Taek-Mo Chung *[ab] and Bo Keun Park *[ab]

Received 14th June 2020
Accepted 3rd August 2020

DOI: 10.1039/d0ra05225f

rsc.li/rsc-advances

Heteroleptic manganese compounds, $[Mn(tmhd)(TMEDA)Cl]_2$ (**1**), $[Mn(tmhd)(dmamp)]_2$ (**2**), $Mn_2(tmhd)_2(edpa)_2(\mu\text{-THF})$ (**3**), $[Mn(dmampea)(NEt_2)]_2$ (**4**), and Mn(dmampea)(^{i}Pr-MeAMD) (**5**), were synthesized and characterized. Compound **5** was a volatile liquid. Structural analysis revealed that **1–4** were dimers. Compounds **1** and **3**, **2**, and **4** had distorted octahedral, distorted trigonal-bipyramidal, and distorted tetrahedral geometries around the Mn centers, respectively. Based on thermogravimetric analysis, the residues of **2** and **3** were expected to be MnO and Mn_3O_4, respectively. According to thermogravimetric analysis, **4** showed a higher residual value, whereas **5** exhibited a lower value than those expected for manganese nitrides.

Introduction

Manganese is an important component in several classes of materials, such as solid electrolytes in batteries[1] and solid oxide fuel cells[2] as well as magnetoresistive oxides,[3] magnetic materials,[4] supercapacitors,[5] catalysts,[6] and microelectronics.[7] Manganese-based thin films have been deposited *via* several methods, including liquid-phase electrochemical methods,[8] physical vapor deposition (PVD),[4f,5b,c,9] molecular beam epitaxy (MBE),[4a,b,d,10] chemical vapor deposition (CVD),[2a,3,11] and atomic layer deposition (ALD).[7c,12] The CVD and ALD processes are useful to form large-area thin films of good uniformity using metal precursors. Furthermore, through ALD techniques, highly uniform thin films can be formed on very high aspect ratio structures. The success of the CVD and ALD processes critically depends on the availability of volatile and thermally stable precursors. The ideal precursors must have high vapor pressure, high volatility, high purity, low deposition temperature, high deposition rate, chemical and thermal stability during transportation, low cost, and a simple reaction path to deposition. Moreover, they must allow high control over composition, easy handling, easy treatment, and easy removal of byproducts.

Manganese-containing thin films have been deposited by CVD and ALD from $Mn(tmhd)_3$,[2a,3,11a,c,d,e,12c] $MnCp_2$,[11f] $Mn(EtCp)_2$,[11f,j,12a] $Mn(CpR)(CO)_3$,[11f,h,l] $Mn(hfa)_2\cdot TMEDA$,[11i,n] $Mn(N^tBu_2)_2$,[11k] bis(2,2,6,6-tetramethylpiperidido)manganese(II),[11m] $Mn(N,N'\text{-di-isopropylpentylamidinato})_2$,[11g,h] and $Mn(OCRR'CN^tBu)_2$.[12b] However, new manganese precursors must be developed because of the thermal instability, low shelf life, and low vapor pressures of the existing precursors.

Our group has studied the applications of CVD and ALD and the syntheses of metal precursors that contain an aminoalkoxide group, in which the two alkyl groups positioned on the α-carbon of the hydroxyl group are substituted, and exhibit improved volatility[13] as well as *N*-alkoxy carboxamides having adjusted both sides of the amide group.[14] Recently, we investigated the syntheses and applications of heteroleptic precursors with two distinct ligands attached to the metal center. A heteroleptic precursor may lead to improved volatility, stability, and reactivity compared to homoleptic precursors that contain the same ligands. Also, we are studying a precursor that contains an aminoamide ligand that was formed by substituting the hydroxyl group of the aminoalkoxide moiety with an amide group.

In this paper, we report the synthesis of $[Mn(tmhd)(TMEDA)Cl]_2$ (**1**) (tmhd = 2,2,6,6-tetramethyl-3,5-heptanedionate, TMEDA = *N*,*N*,*N*′,*N*′-tetramethylethylenediamine), $[Mn(tmhd)(dmamp)]_2$ (**2**) (dmamp = 1-dimethylamino-2-methyl-2-propoxide), $Mn_2(tmhd)_2(edpa)_2(\mu\text{-THF})$ (**3**) (edpa = *N*-ethoxy-2,2-dimethylpropanamide), $[Mn(dmampea)(NEt_2)]_2$ (dmampea = (1-(dimethylamino)-2-methylpropan-2-yl)(ethyl)amide) (**4**), and Mn(dmampea)(^{i}Pr-MeAMD) (^{i}Pr-MeAMD = *N*,*N*′-diisopropylacetamidinate) (**5**) as heteroleptic precursors for the preparation of thin films containing manganese. These compounds were

[a]*Thin Film Materials Research Center, Korea Research Institute of Chemical Technology (KRICT), 141 Gajeong-Ro, Yuseong-Gu, Daejeon 34114, Republic of Korea. E-mail: tmchung@krict.re.kr; parkbk@krict.re.kr*

[b]*Department of Chemical Convergence Materials, University of Science and Technology (UST), 217, Gajeong-Ro, Yuseong-Gu, Deajeon 34113, Republic of Korea*

† Electronic supplementary information (ESI) available: Molecular structure of molecules 1 and 2 in the asymmetric unit of 4 (Fig. S1). CCDC 2002601–2002604. For ESI and crystallographic data in CIF or other electronic format see DOI: 10.1039/d0ra05225f

characterized *via* infrared (IR) spectroscopy and microanalysis as well as single-crystal X-ray diffraction analysis.

Experimental

General comments

All reactions were carried out under inert dry conditions using standard Schlenk line techniques or in an argon-filled glove box. Tetrahydrofuran (THF), hexane, and toluene solvents were purified using the Innovative Technology PS-MD-4 solvent-purification system. Moreover, Na(dmamp),[13b] edpaH,[14a] and Li(^{i}Pr-MeAMD)[15] were synthesized *via* the referenced modified methods. All other chemicals were purchased from Aldrich. IR spectra were obtained using a Nicolet Nexus Fourier-transform IR (FT-IR) spectrophotometer. Elemental analysis was conducted using the Thermo Scientific Flash 2000 Organic Elemental Analyzer. Thermogravimetric analysis (TGA) was performed using a Setaram TG/DTA 92-18 instrument.

Synthesis of Na(edpa)

First, edpaH (1.0 g, 6.7 mmol) was added dropwise to a NaH (0.16 g, 6.9 mmol) suspension in toluene (100 mL). After reacting for 12 h, the mixture was filtered. A white powder was obtained *via* evaporation of the filtrate *in vacuo*. Yield: 0.95 g (84%). ^{1}H NMR (C_6D_6, 400 MHz): δ 1.26 (t, J = 8.00 Hz, 3H, –OCH$_2$CH_3), 1.30 (S, 9H, –C(CH_3)$_3$), 3.22 (q, J = 8.00, 2H, –OCH_2CH$_3$).

Synthesis of Li(dmampea)

Isobutylene oxide (35 mL, 0.39 mol) was added dropwise to dimethylamine (50 mL of 40 wt% solution in H_2O, 0.39 mol) under ice-water cooling, and the reaction mixture was stirred at ambient temperature for 12 h. Diethyl ether (200 mL) and water (200 mL) were added to the solution. The organic layer was separated, and the aqueous layer was extracted with diethyl ether (2 × 200 mL). The combined organic layer was dried over $MgSO_4$ and filtered. Purification *via* distillation (110 °C) afforded 1-(dimethylamino)-2-methylpropan-2-ol as a colorless oil. Yield: 40 g (89%). ^{1}H NMR ($CDCl_3$, 400 MHz): δ 1.16 (s, 6H, –C(CH_3)$_2$), 2.27 (s, 2H, –CH_2–), 2.36 (s, 6H, –N(CH_3)$_2$).

Concentrated sulfuric acid (60 mL) was slowly added to stirred acetonitrile (200 mL) at 0 °C. The resulting solution was added dropwise to a mixture of 1-(dimethylamino)-2-methylpropan-2-ol (5 g, 42.69 mmol) in acetonitrile (200 mL) at 0 °C. The reaction mixture was stirred at room temperature for 2 days, and then crushed ice was poured onto the mixture. The reaction mixture was subjected to reduced pressure to evaporate acetonitrile, cooled in an ice bath, and basified with an aqueous sodium hydroxide solution to adjust the pH to 10. The mixture was extracted three times with diethyl ether. The combined organic layer was washed with water, dried over $MgSO_4$, and concentrated to afford *N*-(1-(dimethylamino)-2-methylpropan-2-yl) acetamide as a light-yellow oil. Yield: 3.23 g (45%). ^{1}H NMR ($CDCl_3$, 400 MHz): δ 1.33 (s, 6H, –C(CH_3)$_2$), 1.93 (s, 3H, –CCH_3), 2.32 (s, 6H, –N(CH_3)$_2$), 2.41 (s, 2H, –CH_2–).

Lithium aluminum hydride 15.0 g (0.06 mol) was suspended in THF (100 mL) under ice-water cooling, the mixture was stirred for 1 h, and *N*-(1-(dimethylamino)-2-methylpropan-2-yl) acetamide (3.23 g, 0.02 mol) in THF was slowly added. The mixture was stirred for 12 h under reflux, the temperature was reduced to room temperature, and water (3 mL) and a 10% aqueous sodium hydroxide solution (15 mL) were added dropwise to the reaction mixture under ice-water cooling. After the removal of the insoluble fraction *via* filtration, the filtrate was dried over anhydrous $MgSO_4$, and the solvent was removed *via* distillation under reduced pressure to afford N_2-ethyl-N_1,N_1,2-trimethylpropane-1,2-diamine. Yield: 2.23 g (98%). ^{1}H NMR ($CDCl_3$, 400 MHz): δ 1.02 (s, 6H, –C(CH_3)$_2$), 1.09 (t, J = 7.12 Hz, 3H, –CH$_2$CH_3), 2.22 (s, 2H, –NCH_2–), 2.31 (s, 6H, –N(CH_3)$_2$), 2.54 (q, J = 7.16 Hz 2H, –NHCH_2–).

Furthermore, ^{n}BuLi (2.7 mL) was added dropwise to a solution of N_2-ethyl-N_1,N_1,2-trimethylpropane-1,2-diamine (1.0 g, 7.0 mmol) in THF (50 mL) at 0 °C and the reaction mixture was stirred for 12 h. The solvent of the mixture was removed *in vacuo* to obtain lithium (1-(dimethylamino)-2-methylpropan-2-yl) (ethyl)amide (Li(dmampea)) as a yellow powder. This compound was used without further purification.

Synthesis of [Mn(tmhd)(TMEDA)Cl]$_2$ (1)

Na(tmhd) (0.82 g, 4.0 mmol) was added to a solution of $MnCl_2$ (0.50 g, 4.0 mmol) and TMEDA (0.46 g, 4.0 mmol) in THF (30 mL). After stirring the mixture for 12 h, the solvent was removed *in vacuo*. The residues were extracted with hexane and filtered. The crude product was obtained *via* evaporation of the filtrate *in vacuo*, and it was purified *via* recrystallization from toluene at room temperature to afford a pure product as yellow crystals. Yield: 1.04 g (67%). FT-IR (KBr, cm^{-1}): 3005 (m), 2961 (s), 2867 (m), 2836 (s), 2796 (m), 1591 (s), 1574 (s), 1535 (s), 1501 (s), 1456 (s), 1415 (s), 1399 (s), 1358 (s), 1287 (m), 1245 (m), 1223 (m), 1182 (w), 1164 (w), 1135 (m), 1065 (w), 1031 (m), 1018 (w), 954 (m), 931 (w), 867 (m), 793 (m), 772 (w), 736 (w), 606 (w), 583 (w), 474 (w), 436 (w); elemental analysis calcd (%) for $Mn_2C_{34}H_{70}Cl_2N_4O_4$: C, 52.37; H, 9.05; N, 7.19; found: C, 55.24; H, 9.90; N, 8.72.

Synthesis of [Mn(tmhd)(dmamp)]$_2$ (2)

Na(tmhd) (0.82 g, 4.0 mmol) was added to a suspension of $MnCl_2$ (0.5 g, 4.0 mmol) in THF (30 mL). After stirring the mixture at room temperature for 6 h, Na(dmamp) (0.55 g, 4.0 mmol) was added and the reaction mixture was stirred for 12 h. The solvent of the mixture was removed *in vacuo*. The residues were extracted with hexane and filtered. The crude product was obtained *via* evaporation of the filtrate *in vacuo*, and it was purified *via* recrystallization from THF at room temperature to afford a pure product as yellow crystals. Yield: 0.99 g (70%). FT-IR (KBr, cm^{-1}): 2962 (s), 2864 (m), 2836 (w), 2791 (w), 1588 (s), 1574 (s), 1549 (m), 1537 (m), 1505 (m), 1452 (w), 1406 (s), 1358 (m), 1246 (w), 1225 (w), 1190 (w), 1162 (w), 1136 (w), 1123 (w), 1034 (w), 1021 (w), 983 (m), 941 (m), 911 (w), 869 (w), 843 (w), 790 (w), 760 (w), 738 (w), 609 (w), 582 (w), 539 (w), 474 (w), 450 (w); elemental analysis calcd (%) for $Mn_2C_{34}H_{66}N_2O_6$: C, 57.62; H, 9.39; N, 3.95; found: C, 57.14; H, 9.55; N, 3.87.

Synthesis of $Mn_2(tmhd)_2(edpa)_2(\mu\text{-THF})$ (3)

Na(tmhd) (0.82 g, 4.0 mmol) was added to a suspension of $MnCl_2$ (0.5 g, 4.0 mmol) in THF (30 mL). After stirring the mixture at room temperature for 6 h, Na(edpa) (0.67 g, 4.0 mmol) was added and the reaction mixture was stirred for 12 h. The solvent of the mixture was removed *in vacuo*. The residues were extracted with hexane and filtered. The crude product was obtained after evaporation of the filtrate *in vacuo*, and it was purified *via* recrystallization from THF at room temperature to obtain a pure product as yellow crystals. Yield: 1.17 g (70%). FT-IR (KBr, cm^{-1}): 2964 (s), 2869 (s), 1589 (s), 1572 (s), 1554 (s), 1539 (s), 1504 (s), 1479 (m), 1459 (w), 1389 (s), 1358 (m), 1324 (w), 1246 (w), 1224 (w), 1187 (m), 1136 (w), 1092 (w), 1055 (s), 956 (w), 935 (w), 899 (m), 868 (s), 792 (w), 762 (w), 737 (w), 612 (w), 537 (w), 525 (w), 492 (w), 474 (w); elemental analysis calcd (%) for $C_{40}H_{74}Mn_2N_2O_9 \cdot H_2O$: C, 56.20; H, 8.96; N, 3.28; found: C, 56.59; H, 8.75; N, 3.67.

Synthesis of $[Mn(dmampea)(NEt_2)]_2$ (4)

Li(dmampea) (0.60 g, 4.0 mmol) was added to a suspension of $MnCl_2$ (0.5 g, 4.0 mmol) in THF (30 mL). After stirring the mixture at room temperature for 6 h, $Li(NEt_2)$ (0.31 g, 4.0 mmol) was added, and the reaction mixture was stirred for 12 h. The solvent of the reaction mixture was removed *in vacuo*. The residues were extracted with hexane and filtered. The crude product was obtained *via* evaporation of the filtrate *in vacuo*, and it was purified *via* recrystallization from toluene at room temperature to afford a pure product as brown crystals. Yield: 0.75 g (69%). FT-IR (KBr, cm^{-1}): 2962 (s), 2926 (s), 2861 (s), 2598 (w), 1648 (w), 1497 (s), 1377 (m), 1359 (m), 1330 (m), 1313 (m), 1261 (m), 1206 (m), 1173 (m), 1121 (w), 1044 (w), 1015 (w), 941 (w), 877 (w), 840 (w), 807 (w), 624 (w), 574 (w); elemental analysis calcd (%) for $C_{24}H_{58}Mn_2N_6 \cdot 2H_2O$: C, 49.99; H, 10.84; N, 14.57; found: C, 49.57; H, 10.16; N, 14.81.

Synthesis of Mn(dmampea)(^{i}Pr-MeAMD) (5)

Li(dmampea) (0.60 g, 4.0 mmol) was added to a suspension of $MnCl_2$ (0.5 g, 4.0 mmol) in THF (30 mL). After stirring the mixture at room temperature for 6 h, Li(^{i}Pr-MeAMD) (0.59 g, 4.0 mmol) was added and the reaction mixture was stirred for 12 h. The solvent of the reaction mixture was removed *in vacuo*. The residues were extracted with hexane and filtered. The crude product was obtained *via* evaporation of the filtrate *in vacuo*, and it was purified *via* distillation at 110 °C under a reduced pressure of 10^{-1} Torr to obtain a pure product as a yellow liquid. Yield: 0.54 g (40%). FT-IR (KBr, cm^{-1}): 2961 (s), 2927 (s), 2862 (s), 2787 (w), 2600 (w), 1650 (w), 1496 (s), 1376 (s), 1357 (s), 1314 (s), 1261 (w), 1204 (m), 1173 (m), 1150 (m), 1121 (m), 1083 (w), 1050 (m), 1014 (w), 939 (w), 876 (w), 804 (w), 731 (w); elemental analysis calcd (%) for $C_{16}H_{37}MnN_4$: C, 56.45; H, 10.96; N, 16.46; found: C, 56.40; H, 10.57; N, 16.29.

X-ray crystallography

Crystals of **1** suitable for X-ray analysis were obtained *via* recrystallization from toluene at room temperature. Crystals of **2** and **3** were grown from a saturated THF solution at room temperature. Crystals of **4** were isolated *via* recrystallization from hexane. A specimen of suitable size and quality was coated with Paratone oil and mounted onto a glass capillary. Reflection data were collected using a Bruker Apex II-CCD area-detector diffractometer with graphite-monochromated MoKα radiation (λ = 0.71073 Å). The hemisphere of reflection data were collected as ω scan frames with 0.3° per frame and an exposure time of 10 s per frame. Cell parameters were determined using the SMART program[16] and refined with SAINT software.[17] Data reduction was performed using SAINT software.[17] The data were corrected for the Lorentz and polarization effects. Absorption correction was applied using the SADABS program.[18] The structures were solved *via* direct methods and all nonhydrogen atoms were subjected to anisotropic refinement *via* full-matrix least-squares on F^2 using the SHELXTL/PC package.[19] Hydrogen atoms were placed at their geometrically calculated positions and refined on the corresponding carbon atoms using the riding model with isotropic thermal parameters. CCDC 2002604 (**1**), CCDC 2002602 (**2**), CCDC 2002603 (**3**), and CCDC 2002601 (**4**) contain supplementary crystallographic data.†

Thermal analysis

TGA and differential thermal analysis (DTA) for the newly synthesized compounds were performed using the Setaram TG/

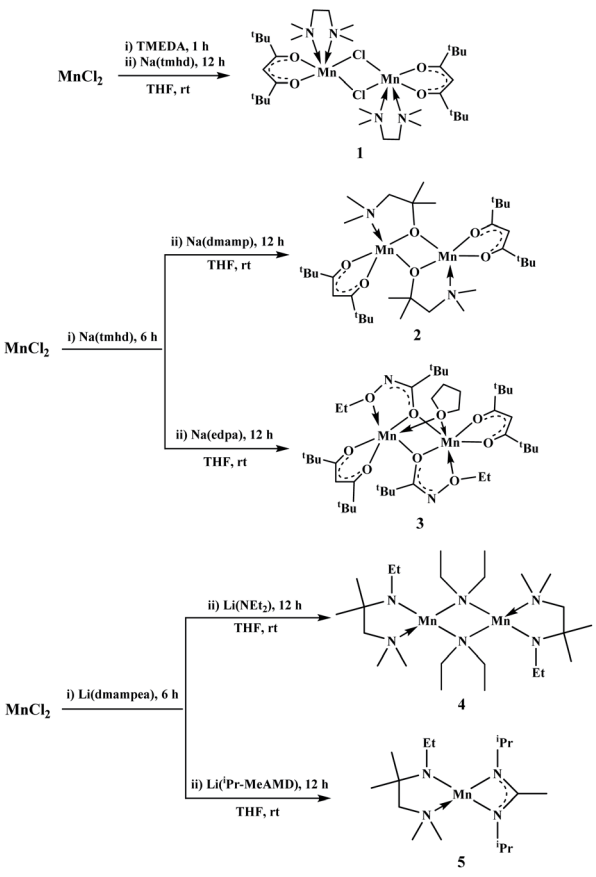

Scheme 1 Synthesis of compounds 1–5.

DTA 92-18 instrument. The TG data of the compounds were obtained up to 800 °C at a heating rate of 10 °C min^{-1} under atmospheric pressure with N_2 as a carrier gas. TG sampling was carried out inside an argon-filled glove box to avoid air contact. However, the samples were exposed to air for less than 1 min when setting them in the TGA apparatus.

Results and discussion

The reaction of $MnCl_2$ with 1 equiv. of Na(tmhd) in the presence of 1 equiv. TMEDA afforded manganese(II) compound **1** in 67% yield (Scheme 1). After mixing $MnCl_2$ with 1 equiv. of Na(tmhd) in THF for 6 h, the mixture was treated with 1 equiv. of Na(dmamp) and Na(edpa), and it afforded **2** (76%) and **3** (69%), respectively (Scheme 1).

After the reaction of $MnCl_2$ with 1 equiv. of Li(dmampea), which is an aminoamide ligand, for 6 h in THF and treatment of the mixture with 1 equiv. of $Li(NEt_2)$ and Li(^{i}Pr-MeAMD), we obtained **4** (69%), and **5** (40%), respectively. Compound **5** was liquid and vaporized well when distilled at 110 °C under a reduced pressure of 10^{-1} Torr.

The compounds had good solubility in organic solvents, such as toluene, hexane, and diethyl ether under inert conditions.

The crystals of **1–3** were obtained from saturated solutions of toluene (for **1**) and THF (for **2** and **3**) at room temperature. The crystal of **2** exhibited thermal disorder with the tmhd ligand. The crystallographic data are summarized in Table 1. Selected bond lengths and angles of **1–3** are listed in Table 2.

The crystals of **1–3** formed dimeric structures through the two Cl atoms (for **1**), two O atoms of the two dmamp ligands (for **2**), and two O atoms of the two edpa ligands and one O atom of THF (for **3**). The crystal structures of **1** and **3** had a distorted octahedral geometry around each central Mn atom, unlike **2** which had a distorted trigonal-bipyramidal geometry (Fig. 1–3). Compound **3** was expected to be a 5-coordinated molecule like **2**; however, it had a distorted octahedral geometry with 6-coordination, which contained the O atom of the THF molecule bridged to the two Mn atoms. A possible reason for this behavior is that the edpa ligand was sterically smaller than the dmamp ligand because the backbone of edpa was planar due to the double bond character.

In **1–3**, the tmhd ligands were bonded to the Mn atoms that formed six-membered metallacycles: Mn1–O1–C1–C2–C3–O2 with an O1–Mn1–O2 bite angle of 83.48(3)° for **1**, Mn1–O1–C1–C2–C3–O2 with an O1–Mn1–O2 bite angle of 84.80(6)° for **2**, and Mn1–O3–C8–C9–C10–O4 and Mn11–O13–C28–C29–C30–O14 with O3–Mn1–O4 and O13–Mn11–O14 bite angles of 86.47(15)° and 86.21(3)°, respectively, for **3**. The lengths of the Mn1–O1 and Mn1–O2 bonds (tmhd) were 2.1109(8) and 2.1141(8) Å in **1**, and 2.0868(15) and 2.0959(16) Å in **2**, respectively. In **3**, the lengths of the Mn1–O3, Mn1–O4, Mn11–O13, and Mn11–O14 bonds were 2.074(4), 2.092(4), 2.076(4), and 2.084(4) Å, respectively. The bond lengths and angles tended to move oppositely; *i.e.*, **1** had the longest bonds and smallest bond angles.

Table 1 Crystallographic data and data collection parameters for **1–4**

	1	**2**	**3**	**4**
Formula weight	779.72	710.78	838.91	540.64
Crystal system	Monoclinic	Monoclinic	Monoclinic	Triclinic
Space group	$P2_1/c$	$P2_1/n$	$P2_1/c$	$P\bar{1}$
Temperature (K)	100(1)	100(1)	100(1)	100(1)
Wavelength (Å)	0.71073	0.71073	0.71073	0.71073
a (Å)	10.3578(3)	10.1761(4)	12.7642(5)	9.6293(3)
b (Å)	18.3221(5)	9.1185(4)	21.0617(9)	11.7366(4)
c (Å)	11.8508(3)	21.7996(9)	17.1722(8)	13.3435(4)
α (°)	90	90	90	95.882(2)
β (°)	111.7850(10)	93.970(2)	90.417(2)	92.369(2)
γ (°)	90	90	90	91.115(2)
Volume (Å^3)	2088.39(10)	2017.95(15)	4616.4(3)	1498.37(8)
Z	2	2	4	2
P_{calcd} (Mg m^{-3})	1.240	1.170	1.207	1.198
μ (mm^{-1})	0.770	0.665	0.596	0.864
F (000)	836	768	1808	588
Crystal size (mm^3)	0.20 × 0.18 × 0.09	0.20 × 0.12 × 0.08	0.20 × 0.12 × 0.04	0.70 × 0.34 × 0.26
Theta range (°)	2.12–28.40	1.87–28.31	1.53–28.27	1.54–26.00
Index ranges	$-13 \le h \le 12$	$-13 \le h \le 13$	$-16 \le h \le 16$	$-11 \le h \le 11$
	$0 \le k \le 24$	$0 \le k \le 12$	$0 \le k \le 28$	$-14 \le k \le 14$
	$0 \le l \le 15$	$0 \le l \le 28$	$0 \le l \le 22$	$0 \le l \le 16$
Indep. refl.	5228	4994	11 322	5882
GOF on F^2	1.080	1.052	1.091	1.063
R_1 $[I > 2\sigma(I)]^a$	0.0253	0.0479	0.0951	0.0492
wR_2 (all data)^b	0.0635	0.1483	0.2593	0.1286

^{a} $R_1 = (\Sigma||F_o| - |F_c||)/\Sigma|F_o|$. ^{b} w$R_2 = [\Sigma\omega(F_o^2 - F_c^2)^2/\Sigma\omega(F_o^2)^2]^{1/2}$.

Compounds **1–3** contained four-membered rings that were formed by the atoms bridged between the two Mn atoms (Cl for **1**, O for **2** and **3**). For **1**, the four-membered ring Mn1–Cl1–$Mn1^{i}$–$Cl1^{i}$ had bond angles of 94.127(10)° (Mn1–Cl1–$Mn1^{i}$) and 85.872(10)° (Cl1–Mn1–$Cl1^{i}$) and bond lengths of 2.5343(3) Å (Mn1–Cl1) and 2.5310(3) Å (Mn1–$Cl1^{i}$), which were in similar to those of the Mn–Cl bridging compounds.[20] Compounds **2** and **3** formed four-membered rings with the O atoms of the two dmamp and edpa ligands, respectively. The bond angles of the Mn1–O3–$Mn1^{i}$–$O3^{i}$ ring in **2** were 84.85(6)° (O3–Mn1–$O3^{i}$) and 95.15(6)° (Mn1–O3–$Mn1^{i}$), whereas those of the Mn1–O2–Mn11–O12 ring in **3** were 81.61(14)° (O2–Mn1–O12), 81.31(14)°

Table 2 Selected bond lengths (Å) and bond angles (°) for **1–3**

Bond lengths (Å)

1		**2**		**3**	
Mn(1)–O(1)	2.1109(8)	Mn(1)–O(1)	2.0868(15)	Mn(1)–O(1)	2.229(4)
Mn(1)–O(2)	2.1141(8)	Mn(1)–O(2)	2.0959(16)	Mn(1)–O(2)	2.146(4)
Mn(1)–N(1)	2.3443(10)	Mn(1)–O(3)	2.0592(17)	Mn(1)–O(3)	2.074(4)
Mn(1)–N(2)	2.3866(11)	Mn(1)–$O(3)^{i}$	2.1097(14)	Mn(1)–O(4)	2.092(4)
Mn(1)–Cl(1)	2.5343(3)	Mn(1)–N(1)	2.3106(18)	Mn(1)–O(5)	2.578(4)
Mn(1)–$Cl(1)^{i}$	2.5310(3)			Mn(1)–O(12)	2.149(4)
				Mn(11)–O(11)	2.203(4)
				Mn(11)–O(12)	2.162(4)
				Mn(11)–O(13)	2.076(4)
				Mn(11)–O(14)	2.084(4)
				Mn(11)–O(2)	2.147(4)
				Mn(11)–O(5)	2.455(4)
Mn(1)⋯$Mn(1)^{i}$	3.7084(3)	Mn(1)⋯$Mn(1)^{i}$	3.0774(6)	Mn(1)⋯Mn(11)	3.112(1)

Bond angles (°)

1		**2**		**3**	
O(1)–Mn(1)–O(2)	83.48(3)	O(1)–Mn(1)–O(2)	84.80(6)	O(3)–Mn(1)–O(4)	86.47(15)
O(1)–Mn(1)–N(1)	86.01(3)	O(3)–Mn(1)–O(1)	112.91(6)	O(3)–Mn(1)–O(2)	152.89(15)
O(1)–Mn(1)–N(2)	91.03(4)	O(3)–Mn(1)–O(2)	109.92(7)	O(4)–Mn(1)–O(2)	111.30(15)
O(2)–Mn(1)–N(2)	86.70(4)	O(1)–Mn(1)–N(1)	141.27(7)	O(3)–Mn(1)–O(12)	115.49(16)
O(2)–Mn(1)–N(1)	161.21(4)	O(2)–Mn(1)–N(1)	85.72(7)	O(4)–Mn(1)–O(12)	102.40(15)
N(1)–Mn(1)–N(2)	77.95(4)	O(3)–Mn(1)–N(1)	105.64(7)	O(2)–Mn(1)–O(12)	81.61(14)
O(1)–Mn(1)–Cl(1)	178.11(3)	O(1)–Mn(1)–$O(3)^{i}$	101.30(6)	O(3)–Mn(1)–O(1)	86.26(15)
O(2)–Mn(1)–Cl(1)	95.39(2)	O(2)–Mn(1)–$O(3)^{i}$	160.62(7)	O(4)–Mn(1)–O(1)	103.08(17)
N(1)–Mn(1)–Cl(1)	95.48(3)	O(3)–Mn(1)–$O(3)^{i}$	84.85(6)	O(2)–Mn(1)–O(1)	70.23(14)
N(2)–Mn(1)–Cl(1)	90.42(3)	$O(3)^{i}$–Mn(1)–N(1)	78.02(6)	O(12)–Mn(1)–O(1)	147.30(16)
O(1)–Mn(1)–$Cl(1)^{i}$	92.91(3)	Mn(1)–O(3)–$Mn(1)^{i}$	95.15(6)	O(5)–Mn(1)–O(2)	74.29(13)
O(2)–Mn(1)–$Cl(1)^{i}$	103.64(3)			O(5)–Mn(1)–O(12)	71.86(14)
N(1)–Mn(1)–$Cl(1)^{i}$	92.38(3)			O(5)–Mn(1)–O(1)	84.48(15)
N(2)–Mn(1)–$Cl(1)^{i}$	169.28(3)			O(5)–Mn(1)–O(3)	90.64(14)
Cl(1)–Mn(1)–$Cl(1)^{i}$	85.872(10)			O(5)–Mn(1)–O(4)	171.70(14)
Mn(1)–Cl(1)–$Mn(1)^{i}$	94.127(10)			O(13)–Mn(11)–O(14)	86.21(15)
				O(13)–Mn(11)–O(2)	117.10(15)
				O(14)–Mn(11)–O(2)	100.20(15)
				O(13)–Mn(11)–O(12)	151.25(15)
				O(14)–Mn(11)–O(12)	113.41(15)
				O(2)–Mn(11)–O(12)	81.31(14)
				O(13)–Mn(11)–O(11)	87.85(15)
				O(14)–Mn(11)–O(11)	93.81(17)
				O(2)–Mn(11)–O(11)	151.91(15)
				O(12)–Mn(11)–O(11)	70.77(14)
				O(13)–Mn(11)–O(5)	88.07(14)
				O(14)–Mn(11)–O(5)	171.57(15)
				O(2)–Mn(11)–O(5)	76.96(14)
				O(12)–Mn(11)–O(5)	74.23(14)
				O(11)–Mn(11)–O(5)	92.16(15)
				Mn(1)–O(2)–Mn(11)	92.93(15)
				Mn(1)–O(12)–Mn(11)	92.43(15)
				Mn(1)–O(5)–Mn(11)	76.35(11)

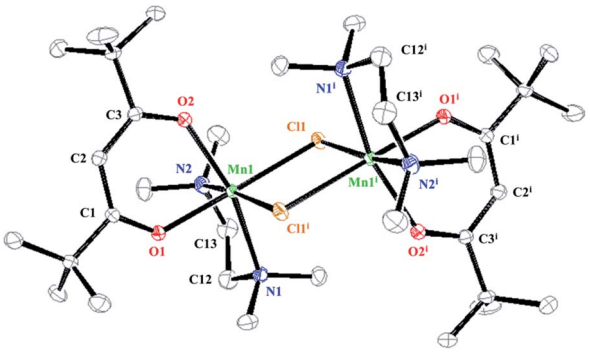

Fig. 1 Molecular structure of **1**. Ellipsoids are set at 50% probability. H atoms omitted for clarity.

(O2–Mn11–O12), 92.93(15)° (Mn1–O2–Mn11), and 92.43° (Mn1–O12–Mn11). The Mn–O lengths were 2.0592(17) Å (Mn1–O3) and 2.1097(14) Å (Mn1–O3^{i}) for **2**, and 2.146(4) Å (Mn1–O2), 2.147(4) Å (Mn11–O2), 2.149(4) Å (Mn1–O12), and 2.162(4) Å (Mn11–O12) for **3**. The bond lengths and angles for **2** and **3** were similar to those of previously reported compounds.[21] The four-membered metallacycles of **1** and **2** were flat because of the inversion centers; however, those of **3** was a butterfly form because of the bonded THF. In **3**, the bond angle of the O atom of the bridged THF molecule with the two Mn atoms was 76.35(11)° (Mn1–O5–Mn11), and the coordinated bond lengths of Mn1–O5 and Mn11–O5 were 2.578(4) and 2.455(4) Å, respectively. The angle between the two planes (Mn1–O2–O12 and Mn11–O2–O12) of the butterfly form was 34.63(9)°.

In **1–3**, the TMEDA, dmamp, and edpa ligands that were bonded to the Mn atoms afforded the five-membered metallacycles Mn1–N1–C12–C13–N2 (for **1**), Mn1–O3^{i}–C12–C13–N1 (for **2**), and Mn1–O1–N1–C1–O2 and Mn11–O11–N11–C21–O12 (for **3**), with bite angles of 77.95(4)° (N1–Mn–N2), 78.02(6)° (O3^{i}–Mn1–N1), and 70.23(14)° (O1–Mn1–O2) and 70.77(14)° (O11–Mn11–O12), respectively. The lengths of the coordinated bonds were 2.3443(10) (Mn1–N1) and 2.3866(11) Å (Mn1–N2) for **1**, 2.3106(18) Å (Mn1–N1) for **2**, and 2.229(4) (Mn1–O1) and 2.203 Å (Mn11–O11) for **3**.

The distance between the two Mn atoms, Mn···Mn (3.7084(3) Å) for **1** was longer than those for **2** and **3** (3.0774(6) Å and 3.112(1) Å, respectively) because of the large size of bridging Cl.

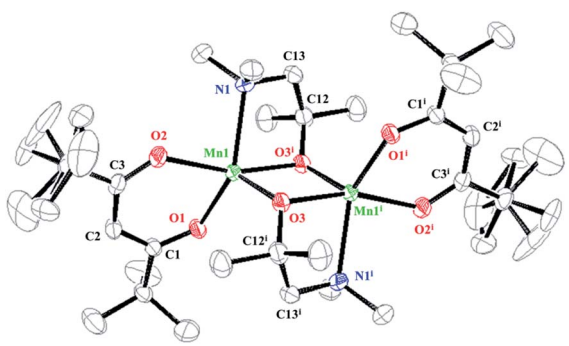

Fig. 2 Molecular structure of **2**. Ellipsoids are set at 50% probability. H atoms omitted for clarity.

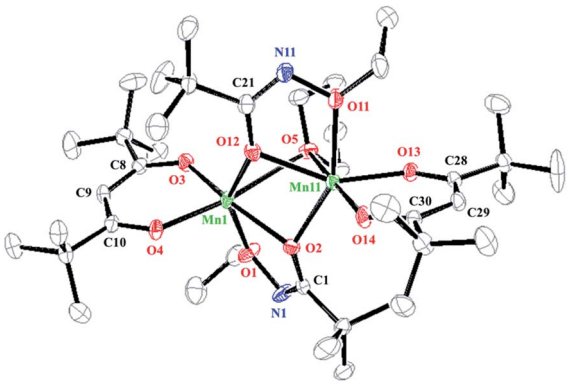

Fig. 3 Molecular structure of **3**. Ellipsoids are set at 50% probability. H atoms omitted for clarity.

The crystals of **4** were obtained from saturated hexane. Compound **4** crystallized with two molecules in the asymmetric unit. Each molecule exhibited slightly different bond lengths and angles. Details of the crystallographic data are summarized in Table 1. Selected bond lengths and angles of **4** are listed in Table 3.

The crystal structure of **4** was dimeric with distorted tetrahedral geometry around each central Mn atom (Fig. 4). The two N atoms of the NEt_2 ligands were bridged between the two Mn atoms, and the two dmampea ligands were combined to one Mn atom in a chelating form (Fig. 4).

The dmampea ligand and Mn atom formed the five-membered metallacycles Mn1–N1–C1–C2–N2 for molecule 1 and Mn2–N4–C4–C5–N5 for molecule 2. The bite angles of molecules 1 and 2 were 82.51(10)° (N1–Mn1–N2) and 82.70(10)° (N4–Mn2–N5), respectively. The lengths of the Mn–N coordination bonds of **4** were 2.250(3) (Mn1–N1) for molecule 1 and 2.260(3) Å (Mn2–N4) for molecule 2. The Mn–N terminal bond

Table 3 Selected bond lengths (Å) and bond angles (°) for **4**

Bond lengths (Å)			
Molecule 1		Molecule 2	
Mn(1)–N(1)	2.250(3)	Mn(2)–N(4)	2.260(3)
Mn(1)–N(2)	2.023(2)	Mn(2)–N(5)	2.019(3)
Mn(1)–N(3)	2.143(2)	Mn(2)–N(6)	2.142(2)
Mn(1)–N(3)^{i}	2.143(2)	Mn(2)–N(6)^{i}	2.145(2)
Mn(1)···Mn(1)^{i}	2.8868(8)	Mn(2)···Mn(2)^{i}	2.9025(8)
Bond angles (°)			
Molecule 1		Molecule 2	
N(1)–Mn(1)–N(2)	82.51(10)	N(4)–Mn(2)–N(5)	82.70(10)
N(1)–Mn(1)–N(3)	114.78(9)	N(4)–Mn(2)–N(6)	113.25(10)
N(1)–Mn(1)–N(3)^{i}	112.09(9)	N(4)–Mn(2)–N(6)^{i}	114.60(10)
N(2)–Mn(1)–N(3)	123.30(10)	N(5)–Mn(2)–N(6)	126.88(10)
N(2)–Mn(1)–N(3)^{i}	129.20(10)	N(5)–Mn(2)–N(6)^{i}	125.33(10)
N(3)–Mn(1)–N(3)^{i}	95.31(9)	N(6)–Mn(2)–N(6)^{i}	94.78(8)
Mn(1)–N(3)–Mn(1)^{i}	84.69(9)	Mn(2)–N(6)–Mn(2)^{i}	85.22(8)

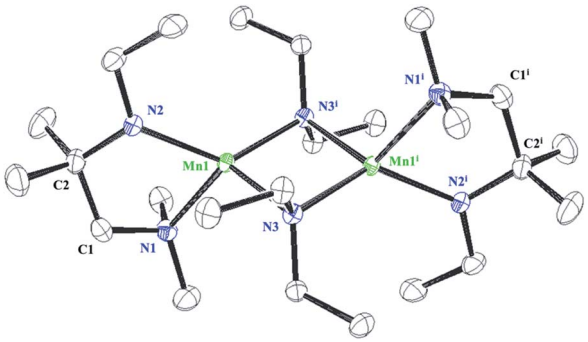

Fig. 4 Molecular structure of molecule 1 in the asymmetric unit of **4**. Ellipsoids are set at 50% probability. H atoms omitted for clarity.

lengths of **4** were 2.023(2) (Mn1–N2) for molecule 1 and 2.019(3) Å (Mn2–N5) for molecule 2.

The four-membered rings that were formed by the two N atoms of the NEt_2 ligands and two Mn atoms, Mn1–N3–Mn1^{i}–N3^{i} and Mn2–N6–Mn2^{i}–N6^{i}, exhibited bond angles of 95.31(9)° (N3–Mn1–N3^{i}) and 84.69(9)° (Mn1–N3–Mn1^{i}) for molecule 1 and 94.78(8)° (N6–Mn2–N6^{i}) and 85.22(8)° (Mn2–N6–Mn2^{i}) for molecule 2. The lengths of the Mn–N bridging bonds of **4** were 2.143(2) (Mn1–N3) and 2.143(2) Å (Mn1–N3^{i}) for molecule 1, and 2.142(2) (Mn2–N6) and 2.145(2) Å (Mn2–N6^{i}) for molecule 2.

The coordinated bonds Mn1–N1 and Mn2–N4 were longer than the other bonds. The lengths of the four bridged bonds (Mn1–N3, Mn1–N3^{i}, Mn2–N6, and Mn2–N6^{i}) were almost the same. The lengths and angles of the Mn–N bridging bonds for reported compounds with amido ligands were 2.078–2.189 Å, and 83.4–88.66° (Mn–N–Mn) and 92.35–96.72° (N–Mn–N).[22]

The distance between the two Mn atoms was 2.8868(8) Å for molecule 1 and 2.9025(8) Å for molecule 2. These distances were shorter than those of **1–3** because if the bulkiness or difference in the bonding formation of the bridging ligand.

All the other bond lengths and angles of **1–4** were within the expected ranges.

TGA curves and weight loss characteristics of **2** and **3** are displayed in Fig. 5. A three-step weight loss was observed for **2**

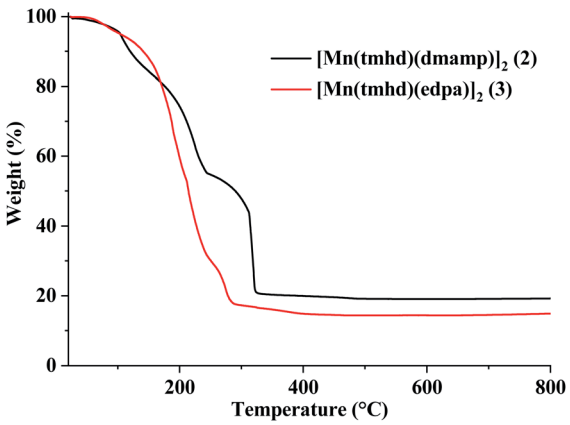

Fig. 5 Thermal analyses of **2** and **3**.

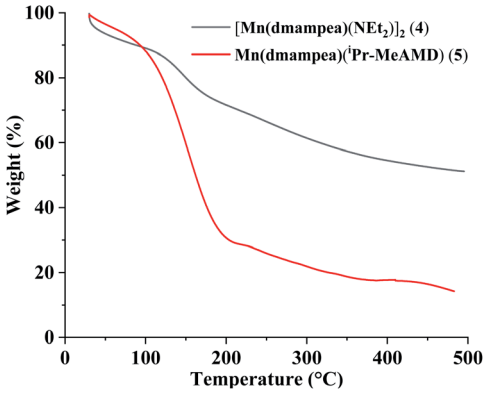

Fig. 6 Thermal analyses of **4** and **5**.

and **3**. For **2**, the first and second weight losses were 8.1% and 26.7% at 100–130 °C and 165–245 °C, respectively. The third part was 30.7% at 280–325 °C. In the case of **3**, the weight losses were 4.3, 63.2, and 10.9% at 50–100, 105–245, and 255–288 °C, respectively. The final residues of **2** and **3** were 20.9% and 17.7%, respectively. The calculated residues for the manganese oxides obtained from **2** and **3** are 20.0 and 17.0, 22.3 and 18.9, 21.5 and 18.2, and 24.5 and 20.8 for MnO, Mn_2O_3, Mn_3O_4, and MnO_2, respectively. The residues of **2** and **3** were expected to be MnO or Mn_3O_4, when compared from the calculated results.

The TGA curves of **4** and **5** were not clear because the compounds were unstable in air for sampling (Fig. 6). Compound **4** showed a continuous weight loss at 25–500 °C. The final residues of **4** were calculated at 51.2%, which was a much higher value than the residual values of known manganese nitrides (Mn_3N_2, Mn_4N, Mn_2N, MnN, Mn_5N_2, *etc.*).

These results suggested that **4** was not volatile and a large amount of decomposed carbon remained in the residue after the thermal decomposition. Conversely, the TGA of **5**, which is a volatile liquid compound, revealed a like single-step weight loss of 68.2% up to 195 °C. The final residues of **5** were calculated at 14.3%, which was a lower value than the expected residual values of manganese nitrides (calculated residue for Mn_3N_2: 18.9; Mn_4N: 22.9; Mn_2N: 18.2; MnN: 40.5; Mn_5N_2: 17.8). The results were indirectly demonstrating that **5** was more volatile than **1–4**.

Among these compounds, **5** was expected to be the best precursor for Mn-containing thin films because it was liquid and had a low evaporation temperature and suitable thermal stability.

Conclusions

We synthesized five heteroleptic compounds, $[Mn(tmhd)(TMEDA)Cl]_2$ (**1**), $[Mn(tmhd)(dmamp)]_2$ (**2**), $Mn_2(tmhd)_2(edpa)_2(\mu\text{-THF})$ (**3**), $[Mn(dmampea)(NEt_2)]_2$ (**4**), and Mn(dmampea)(^{i}Pr-MeAMD) (**5**). Compounds **1–4** were non-volatile solids; however, **5** was a volatile liquid distilled at 110 °C under a reduced pressure of 10^{-1} Torr. Crystallographic studies revealed that **1–4** were dimers bridged by two Cl atoms (for **1**), two O atoms of dmamp (for **2**), two O atoms of edpa and

one O atom of THF (for **3**), and two N atoms of NEt_2 (for **4**); the dimers exhibited distorted octahedral, distorted trigonal bipyramidal, distorted octahedral, and distorted tetrahedral geometries around the Mn centers, respectively. TGA of **2** and **3** showed three-step weight losses and the residues were considered to be MnO and Mn_3O_4, respectively. By TGA, **4** was determined to be thermally unstable because of the significantly higher residue values than the predicted values of known manganese nitrides. The TGA plot of **5** exhibited like single-step weight loss and the residual values were lower than those expected of manganese nitrides. Compound **5** appeared as a useful precursor for Mn-containing thin films because it was liquid and it exhibited low evaporation temperature and suitable thermal stability. We plan to investigate ALD to deposit Mn-containing thin films using **5** as a precursor.

Conflicts of interest

There are no conflicts to declare.

Acknowledgements

This research was supported by a grant from the Development of Organometallics and Device Fabrication for IT ET Convergence Project through the Korea Research Institute of Chemical Technology (KRICT) of Republic of Korea (SI1703-02) and the Development of Smart Chemical Materials for IoT Devices Project through the Korea Research Institute of Chemical Technology (KRICT) of Republic of Korea (SS2021-20).

References

1 (*a*) J. Proell, R. Kohler, A. Mangang, S. Ulrich, C. Ziebert and W. Pfleging, *J. Laser Micro/Nanoeng.*, 2012, **7**, 97–104; (*b*) Y.-H. Liu, S.-S. Liao and B. H. Liu, *Nanoscale*, 2016, **8**, 19978–19983; (*c*) N. Zhang, F. Cheng, J. Liu, L. Wang, X. Long, X. Liu, F. Li and J. Chen, *Nat. Commun.*, 2017, **8**, 405; (*d*) V. Sridhar and H. Park, *J. Alloys Compd.*, 2019, **808**, 151748; (*e*) N. Labyedh, F. Mattelaer, C. Detavernier and P. M. Vereecken, *J. Mater. Chem. A*, 2019, **7**, 18996–19007.

2 (*a*) R. G. Toro, D. M. R. Fiorito, M. E. Fragalà, A. Barbucci, M. P. Carpanese and G. Malandrino, *Mater. Chem. Phys.*, 2010, **124**, 1015–1021; (*b*) J. N. Davis, K. F. Ludwig, K. E. Smith, J. C. Woicik, S. Gopalan, U. B. Pal and S. N. Basu, *J. Electrochem. Soc.*, 2017, **164**, F3091–F3096; (*c*) R. Sažinas, K. B. Andersen, S. B. Simonsen, P. Holtappels and K. K. Hansen, *J. Electrochem. Soc.*, 2019, **166**, F79–F88; (*d*) Y. Zhang, H. Zhao, Z. Du, K. Świerczek and Y. Li, *Chem. Mater.*, 2019, **31**, 3784–3793; (*e*) A. Eksioglu, L. C. Arslan, M. Sezen, C. Ow-Yang and A. Buyukaksoy, *ACS Appl. Mater. Interfaces*, 2019, **11**, 47904–47916.

3 (*a*) T. Nakamura, R. Tai and K. Tachibana, *J. Appl. Phys.*, 2006, **99**, 08Q302; (*b*) T. Nakamura, K. Homma, R. Tai, A. Nishio and K. Tachibana, *IEEE Trans. Magn.*, 2007, **43**, 3070; (*c*) S. Y. Zhou, Y. Zhu, M. C. Langner, Y.-D. Chuang, P. Yu, W. L. Yang, A. G. Cruz Gonzalez, N. Tahir, M. Rini, Y.-H. Chu, R. Ramesh, D.-H. Lee, Y. Tomioka, Y. Tokura, Z. Hussain and R. W. Schoenlein, *Phys. Rev. Lett.*, 2011, **106**, 186404.

4 (*a*) L. W. Guo, H. J. Ko, H. Makino, Y. F. Chen, K. Inaba and T. Yao, *J. Cryst. Growth*, 1999, **205**, 531–536; (*b*) L. W. Guo, D. L. Peng, H. Makino, K. Inaba, H. J. Ko, K. Sumiyama and T. Yao, *J. Magn. Magn. Mater.*, 2000, **213**, 321; (*c*) S. Fujino, M. Murakami, S.-H. Lim, L. G. Salamanca-Riba, M. Wuttig and I. Takeuchi, *J. Appl. Phys.*, 2007, **101**, 013903; (*d*) F. Yu, Y. Liu, M. Yang, S. Wu, W. Zhou and S. Li, *Thin Solid Films*, 2013, **531**, 228–232; (*e*) H. Wang, A. Pomar, S. Martín-Rio, C. Frontera, N. Mestres and B. Martínez, *J. Mater. Chem. C*, 2019, **7**, 12633–12640; (*f*) X. Wang, C. Jin, P. Wang, X. Pang, W. Zheng, D. Zheng, Z. Li, R. Zheng and H. Bai, *Appl. Phys. Lett.*, 2019, **115**, 182405.

5 (*a*) M. Huang, F. Li, F. Dong, Y. X. Zhang and L. L. Zhang, *J. Mater. Chem. A*, 2015, **3**, 21380–21423; (*b*) D. P. M. D. Shaik, P. Rosaiah and O. M. Hussain, *J. Electroanal. Chem.*, 2019, **851**, 113409; (*c*) G. Duraia, P. Kuppusami, T. Maiyalagan, M. Ahila and P. Vinoth kumar, *Ceram. Int.*, 2019, **45**, 17120–17127; (*d*) A. M. Teli, S. A. Bekanalkar, D. S. Patil, S. A. Pawar, T. D. Dongale, J. C. Shin, H. J. Kim and P. S. Patil, *J. Electroanal. Chem.*, 2020, **856**, 113483.

6 (*a*) C.-H. Kuo, I. M. Mosa, A. S. Poyraz, S. Biswas, A. M. El-Sawy, W. Song, Z. Luo, S.-Y. Chen, J. F. Rusling, J. He and S. L. Suib, *ACS Catal.*, 2015, **5**, 1693–1699; (*b*) L. Lu, H. Tian, J. He and Q. Yang, *J. Phys. Chem. C*, 2016, **120**, 23660–23668; (*c*) F. Mattelaer, T. Bosserez, J. Rongé, J. A. Martens, J. Dendooven and C. Detavernier, *RSC Adv.*, 2016, **6**, 98337–98343; (*d*) S. Zhang, B. Zhang, B. Liu and S. Sun, *RSC Adv.*, 2017, **7**, 26226–26242; (*e*) C. Walter, P. W. Menezes, S. Orthmann, J. Schuch, P. Connor, B. Kaiser, M. Lerch and M. Driess, *Angew. Chem., Int. Ed.*, 2018, **57**, 698–702.

7 (*a*) Y. Au, Y. Lin, H. Kim, E. Beh, Y. Liu and R. G. Gordon, *J. Electrochem. Soc.*, 2010, **157**, D341–D345; (*b*) Y. Au, Y. Lin and R. G. Gordon, *J. Electrochem. Soc.*, 2011, **158**, D248–D253; (*c*) V. Selvaraju, A. Brady-Boyd, R. O'Connor, G. Hughes and J. Bogan, *Surf. Interfaces*, 2018, **13**, 133–138 and references therein.

8 (*a*) W. D. Sides and Q. Huang, *Electrochim. Acta*, 2018, **266**, 185–192; (*b*) S. P. Zankowski, L. van Hoecke, F. Mattelaer, M. de Raedt, O. Richard, C. Detavernier and P. M. Vereecken, *Chem. Mater.*, 2019, **31**, 4805–4816; (*c*) C. Rogier, G. Pognon, P. Bondavalli, C. Galindo, G. T. M. Nguyen, C. Vancaeyzeele and P.-H. Aubert, *Surf. Coat. Technol.*, 2020, **384**, 125310.

9 (*a*) M. Aoyama, K. Takenaka and H. Ikuta, *J. Alloys Compd.*, 2013, **577S**, S314–S317; (*b*) K. Kabara and M. Tsunoda, *J. Appl. Phys.*, 2015, **117**, 17B512.

10 (*a*) Y. Yasutomi, K. Ito, T. Sanai, K. Toko and T. Suemasu, *J. Appl. Phys.*, 2014, **115**, 17A935; (*b*) M. Meng, S. X. Wu, L. Z. Ren, W. Q. Zhou, Y. J. Wang, G. L. Wang and S. W. Li, *Appl. Phys. Lett.*, 2015, **106**, 032407; (*c*) T. Gushi, M. J. Klug, J. P. Garcia, S. Ghosh, J.-P. Attané, H. Okuno, O. Fruchart, J. Vogel, T. Suemasu, S. Pizzini and L. Vila, *Nano Lett.*, 2019, **19**, 8716–8723.

11 (*a*) O. Y. Gorbenko, I. E. Graboy, V. A. Amelichev, A. A. Bosak, A. R. Kaul, B. Guttler, V. L. Svetchnikov and H. W. Zandbergen, *Solid State Commun.*, 2002, **124**, 15–20; (*b*) A. W. Topol, K. A. Dunn, K. W. Barth, G. M. Nuesca, B. K. Taylor, K. Dovidenko, A. E. Kaloyeros, R. T. Tuenge and C. N. King, *J. Mater. Res.*, 2004, **19**, 697–706; (*c*) T. Nakamura, R. Tai, T. Nishimura and K. Tachibana, *J. Appl. Phys.*, 2005, **97**, 10H712; (*d*) T. Nakamura, R. Tai, T. Nishimura and K. Tachibana, *J. Electrochem. Soc.*, 2005, **152**, C584–C587; (*e*) R. G. Toro, G. Malandrino, L. M. S. Perdicaro, D. M. R. Fiorito, A. Andreone, G. Lamura and I. L. Fragalà, *Chem. Vap. Deposition*, 2010, **16**, 143–150; (*f*) V. K. Dixit, K. Neishi, N. Akao and J. Koike, *IEEE Trans. Device Mater. Reliab.*, 2011, **11**, 295–302; (*g*) Y. Au, Q. M. Wang, H. Li, J.-S. M. Lehn, D. V. Shenai and R. G. Gordon, *J. Electrochem. Soc.*, 2012, **159**, D382–D385; (*h*) H. Sun and F. Zaera, *J. Phys. Chem. C*, 2012, **116**, 23585–23595; (*i*) Z. Lipani, M. R. Catalano, P. Rossi, P. Paoli and G. Malandrino, *Chem. Vap. Deposition*, 2013, **19**, 22–28; (*j*) N. Jourdan, Y. Barbarin, K. Croes, Y. K. Siew, S. V. Elshocht, Z. Tőkei and E. Vancoille, *ECS Solid State Lett.*, 2013, **2**, P25–P27; (*k*) T. S. Spicer, C. W. Spicer, A. N. Cloud, L. M. Davis, G. S. Girolami and J. R. Abelson, *J. Vac. Sci. Technol., A*, 2013, **31**, 030604; (*l*) K. Assim, J. Jeschke, A. Jakob, D. Dhakal, M. Melzer, C. Georgi, S. E. Schulz, T. Gessner and H. Lang, *Thin Solid Films*, 2016, **619**, 265–272; (*m*) E. Mohimi, B. B. Trinh, S. Babar, G. S. Girolami and J. R. Abelson, *J. Vac. Sci. Technol., A*, 2016, **34**, 060603; (*n*) C. Maccato, L. Bigiani, G. Carraro, A. Gasparotto, R. Seraglia, J. Kim, A. Devi, G. Tabacchi, E. Fois, G. Pace, V. D. Noto and D. Barreca, *Chem. –Eur. J.*, 2017, **23**, 17954–17963.

12 (*a*) B. B. Burton, F. H. Fabreguette and S. M. George, *Thin Solid Films*, 2009, **517**, 5658–5665; (*b*) L. C. Kalutarage, P. D. Martin, M. J. Heeg and C. H. Winter, *J. Am. Chem. Soc.*, 2013, **135**, 12588–12591; (*c*) Y. W. Li, Q. Qiao, J. Z. Zhang, Z. G. Hu and J. H. Chu, *Thin Solid Films*, 2015, **574**, 115–119.

13 (*a*) J. W. Park, H. S. Jang, M. Kim, K. Sung, S. S. Lee, T.-M. Chung, S. Koo, C. G. Kim and Y. Kim, *Inorg. Chem. Commun.*, 2004, **7**, 463–466; (*b*) B. K. Park, H.-S. Kim, S. J. Shin, J. K. Min, K. M. Lee, Y. Do, C. G. Kim and T.-M. Chung, *Organometallics*, 2012, **31**, 8109–8113; (*c*) S. M. George, B. K. Park, C. G. Kim and T.-M. Chung, *Eur. J. Inorg. Chem.*, 2014, 2002–2010; (*d*) J. H. Han, Y. J. Chung, B. K. Park, S. K. Kim, H.-S. Kim, C. G. Kim and T.-M. Chung, *Chem. Mater.*, 2014, **26**, 6088–6091; (*e*) H.-S. Kim, S. M. George, B. K. Park, S. U. Son, C. G. Kim and T.-M. Chung, *Dalton Trans.*, 2015, **44**, 2103–2109; (*f*) S. J. Yeo, B. K. Park, C. G. Kim and T.-M. Chung, *Inorg. Chim. Acta*, 2020, **502**, 119307.

14 (*a*) S. M. George, J. H. Nam, G. Y. Lee, J. H. Han, B. K. Park, C. G. Kim, D. J. Jeon and T.-M. Chung, *Eur. J. Inorg. Chem.*, 2016, 5539–5546; (*b*) J. H. Lee, E. A. Jung, G. Y. Lee, S. H. Han, B. K. Park, S. W. Lee, S. U. Son, C. G. Kim and T.-M. Chung, *ChemistrySelect*, 2018, **3**, 6691–6695.

15 B. S. Lim, A. Rahtu, J.-S. Park and R. G. Gordon, *Inorg. Chem.*, 2003, **42**, 7951–7958.

16 SMART, *version 5.0, Data collection software*, Bruker AXS, Inc., Madison, WI, 1998.

17 SAINT, *version 5.0, Data integration software*, Bruker AXS Inc., Madison, WI, 1998.

18 G. M. Sheldrick, *SADABS, Program for absorption correction with the Bruker SMART system*, Universitat Gottingen, Germany, 1996.

19 G. M. Sheldrick, *SHELXTL*, Bruker AXS Inc., Madison, WI, 1998.

20 (*a*) F. H. Köhler, N. Hebendanz, U. Thewalt, B. Kanellakopulos and R. Klenze, *Angew. Chem.*, 1984, **96**, 697–699; (*b*) E. M. Meyer and C. Floriani, *Angew. Chem.*, 1986, **98**, 376–377; (*c*) F. H. Koehler, N. Hebendanz, G. Mueller, U. Thewalt, B. Kanellakopulos and R. Klenze, *Organometallics*, 1987, **6**, 115–125; (*d*) S. S. Al-Juaid, C. Eaborn, S. M. El-Hamruni, P. B. Hitchcock, J. D. Smith and S. E. S. Can, *J. Organomet. Chem.*, 2002, **649**, 121–127; (*e*) J. Chai, H. Zhu, H. W. Roesky, C. He, H.-G. Schmidt and M. Noltemeyer, *Organometallics*, 2004, **23**, 3284–3289; (*f*) J. Chai, H. Zhu, H. W. Roesky, Z. Yang, V. Jancik, R. Herbst-Irmer, H.-G. Schmidt and M. Noltemeyer, *Organometallics*, 2004, **23**, 5003–5006.

21 (*a*) D. J. Hodgson, B. J. Schwartz and T. N. Sorrell, *Inorg. Chem.*, 1989, **28**, 2226–2228; (*b*) A. Bianchi, L. Calabi, C. Giorgi, P. Losi, P. Mariani, D. Palano, P. Paoli, P. Rossi and B. Valtancoli, *J. Chem. Soc., Dalton Trans.*, 2001, 917–922; (*c*) C. Policar, S. Durot, F. Lambert, M. Cesario, F. Ramiandrasoa and I. Morgenstern-Badarau, *Eur. J. Inorg. Chem.*, 2001, 1807–1818; (*d*) W.-Y. Hsieh, C. M. Zaleski, V. L. Pecoraro, P. E. Fanwick and S. Liu, *Inorg. Chim. Acta*, 2006, **359**, 228–236; (*e*) D. Moon, J. Kim, M. Oh, B. J. Suh and M. S. Lah, *Polyhedron*, 2008, **27**, 447–452; (*f*) X. Jiang, H. Liu, B. Zheng and J. Zhang, *Dalton Trans.*, 2009, 8714–8723.

22 (*a*) A. Belforte, F. Calderazzo, U. Englert, J. Strähle and K. Wurst, *J. Chem. Soc., Dalton Trans.*, 1991, 2419–2427; (*b*) M. A. Putzer, A. Pilz, U. Müller, B. Neumüller and K. Dehnicke, *Z. Anorg. Allg. Chem.*, 1998, **624**, 1336–1340; (*c*) J. Chai, H. Zhu, Q. Ma, H. W. Roesky, H.-G. Schmidt and M. Noltemeyer, *Eur. J. Inorg. Chem.*, 2004, 4807–4811; (*d*) C. Ni, G. J. Long, F. Grandjean and P. P. Power, *Inorg. Chem.*, 2009, **48**, 11594–11600.